Transverse stability of solitary waves propagating in coupled nonlinear dispersive transmission lines

E. Kengne,[1,2,3,*] V. Bozic,[3] M. Viana,[2] and R. Vaillancourt[3]

[1]*Department of Mathematics and Computer Science, Faculty of Science, University of Dschang, P.O. Box 4509, Douala, Republic of Cameroon*

[2]*Institute of Pure and Applied Mathematics, Estrada Dona Castorina 110, 22460-320 Rio de Janeiro, R.J., Brazil*

[3]*Department of Mathematics and Statistics, Faculty of Science, University of Ottawa, 585 King Edward Ave., Ottawa, ON, Canada K1N 6N5*

(Received 4 March 2008; revised manuscript received 7 May 2008; published 11 August 2008)

In the semidiscrete limit and in suitably scaled coordinates, the voltage of a system of coupled nonlinear dispersive transmission lines is described by a nonlinear Schrödinger equation. This equation is used to study the transverse stability of solitary waves of the system. Exact results for the growth rate and the corresponding perturbation function of linear transverse perturbations are obtained in terms of the network's and soliton's parameters.

DOI: 10.1103/PhysRevE.78.026603 PACS number(s): 41.20.Jb, 02.60.Cb

I. INTRODUCTION

Distributed electrical transmission lines that consist of a large number of identical sections have been used for the experimental study of the propagation of KdV solitons which satisfy the famous Korteweg–de Vries equation. This equation was originally derived to model the shallow water wave experiments of John Scott Russel in the 19th century. It is also found in plasmas and dusty plasmas to describe the propagation and interaction of acoustic solitons [1–8]. During the subsequent 40 years our knowledge of solitons has developed to a mature theory. Many soliton equations describing nonlinear systems are known and solitons themselves have been observed (directly or indirectly) in various media. However, there are only a few systems where solitons are easily and directly observed in controlled laboratory experiments. Nonlinear electrical transmission lines are good examples of such systems [9,10]. They are discrete systems but approximate the continuum system quite well, as will be seen below. The nonlinear transmission (NLTLs) provide a useful way to check how the nonlinear excitations behave inside the nonlinear medium and to model the exotic properties of new systems [10]. Let us also point out that, recently, NLTLs have proven to be of great practical use in extremely wideband (frequencies from dc to 100 GHz) focusing and shaping of signals [11] which is usually a hard problem.

The multiplicative process in nonlinear transmission lines is understood as a direct consequence of soliton like propagation in this medium. Qualitatively, the origin of solitons in NLTLs is explained by the balance between the effect of dispersion (due to the periodic location of capacitors in the NLTL) and nonlinearity (due to the voltage dependence of the capacitances). A soliton is a localized wave form that travels along the system with constant velocity and undeformed shape [12]. Physically, signal shaping means changing certain features of incoming signals, such as the frequency content, pulse width, and amplitude. However, all of the above cited studies are limited to a single mode soliton that the single LC transmission line adequately describes in certain parameter regimes, whereas there are many physical phenomena which can be investigated by the use of more than a single electrical transmission line.

To our knowledge, there are only a few works which report on the study of a soliton in the coupled NLTLs. Kakutani *et al.* have [13] theoretically and experimentally reported on the KdV solitons on a coupled LC transmission line consisting of two nonlinear LC ladder lines connected by identical intermediary capacitors and have shown that the network admits two different modes, in each direction of wave propagation. Next, the extension of these studies to envelope solitons has been made by Essimbi *et al.* [14] and Yemele *et al.* [15]. The soliton propagation and interaction on two-dimensional NLTLs have also been studied by Taniuti *et al.* [7].

Extending the transmission line model to higher dimensions has proven to be difficult both theoretically and experimentally. Experiments and resonances of a two-dimensional transmission line have been examined in [16,17] by assuming that the nonlinear capacitance C is of the form $C=\frac{C_0}{1+(V/V_0)^p}$, where V is the voltage in the transmission line, C_0, V_0, and p are all constants. Considering the nonlinear capacitance of the above form, Duan *et al.* [5] have studied the nonlinear waves on coupled nonlinear transmission lines [5]. They found that, in the continuum limit, the voltage for a transmission line is described by a modified Zakharov-Kuznetsov (ZK) equation. The exact cutoff frequencies of the growth rate of the solitary waves for the transverse perturbations have been obtained. Some instability for solitary traveling waves between two cutoff frequencies has been found. In the special case where $p=1$ and in the continuum limit, Kengne *et al.* found that the dynamic of any two wave packets in the nonlinear transmission line is described by coupled nonlinear Schrödinger equations [18]. They derived a set of explicit criteria of modulational (in)stability of the Stokes waves propagating in the lines. In this paper, we as-

*Author to whom correspondence should be addressed; ekengne6@yahoo.fr

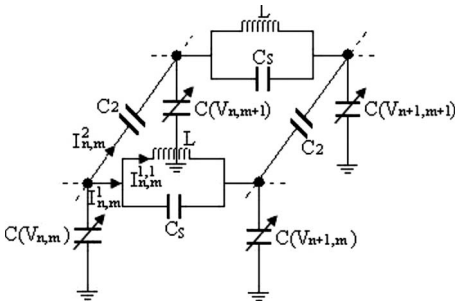

FIG. 1. Part of a system of nonlinear dispersive transmission lines coupled by a capacitor C_2.

sume that the capacitance C is voltage dependent and of a more general form, but only for small-amplitude perturbation voltage, as follows:

$$C(V) = \frac{dQ}{dV} = C_0(1 - 2\alpha V + 3\beta V^2 + \cdots), \tag{1}$$

where C_0 is a constant, V is the perturbation voltage in the transmission line shown in Fig. 1, and α and β are the nonlinear positive coefficients of the electrical charge Q stored in the capacitor of the line. In this paper, we restrict ourselves to the case in which the perturbation voltage V is sufficiently small compared to the equilibrium voltage, so we neglect the higher-order terms in Eq. (1) [19].

The purpose of this work is to conduct the linear stability analysis of solitary waves propagating in coupled nonlinear transmission lines with respect to long-wavelength transverse perturbations on the basis of the nonlinear Schrödinger (NLS) equation. It is well known that the NLS equation is one of the most famous equations in nonlinear science, particularly for the soliton theory. The NLS equation has already been used to study solitary waves propagating in single nonlinear transmission lines (see, for example, Refs. [7,8,20]). The work [7] investigates the NLS equation theoretically, while the works [8,20] experimentally investigate the NLS-type solitons in an electric transmission line. Recently, many researchers have studied the transverse stability of solitary waves on coupled nonlinear transmission lines, using the KdV equation as the governing equation of the network (see, for example, Refs. [4,13,14]), and, to our knowledge, no work has investigated the transverse stability of solitary waves propagating in a coupled NLTLs using the NLS equation as the governing equation. Therefore, our investigation of the transverse perturbations to the two-dimensional NLS equation of the NLTLs may be helpful in other fields of physics.

This paper is organized as follows. In Sec. II, we describe the coupled transmission lines to be studied and write the main circuit equations. In the semidiscrete limit, we show, in Sec. III, that the governing equation of the network can be reduced to a two-dimensional cubic nonlinear Schrödinger equation. The transverse stability of solitons will be investigated in Sec. IV, while the main results are summarized in Sec. V.

II. COUPLED NONLINEAR *LC* DISPERSIVE TRANSMISSION LINES

The basic model used in this work consists of a nonlinear network with many coupled nonlinear *LC* dispersive transmission lines. We imagine that there are many identical dispersive lines [21,22] which are coupled by means of capacitors C_2 at each node, as shown in Fig. 1. Each section of line consists of a constant inductor L in parallel with a linear capacitor C_S (dispersive element) in the series branch and a nonlinear capacitor of capacitance $C=C(V)$ in the shunt branch. The nodes in the system are labeled with two discrete coordinates n and m, where n specifies the nodes in the direction of propagation of the pulse, and m labels the lines in the transverse direction. We apply Kirchhoff's law in the orthogonal loops and obtain the circuit equations for this system as follows:

$$L\frac{\partial I^1_{n,m}}{\partial t} = V_{n,m} - V_{n+1,m}, \tag{2}$$

$$I^2_{n,m} = C_2\frac{d}{dt}(V_{n,m} - V_{n,m+1}),$$

$$I^1_{n,m} - I^{1,1}_{n,m} = C_S\frac{d}{dt}(V_{n-1,m} - V_{n,m}), \tag{3}$$

$$\frac{\partial Q_{n,m}}{\partial t} = I^1_{n-1,m} - I^1_{n,m} + I^2_{n,m-1} - I^2_{n,m}. \tag{4}$$

Therefore, we obtain the circuit equation

$$\frac{\partial^2 Q_{n,m}}{\partial t^2} = \left(\frac{1}{L} + C_S\frac{\partial^2}{\partial t^2}\right)(V_{n-1,m} - 2V_{n,m} + V_{n+1,m}) + C_2\frac{\partial^2}{\partial t^2}(V_{n,m-1} - 2V_{n,m} + V_{n,m+1}). \tag{5}$$

By inserting the above expansion of the capacitance (1) into Eq. (5), we obtain the equation

$$\frac{\partial^2 V_{n,m}}{\partial t^2} + \left(\Omega_0^2 + d_0\frac{\partial^2}{\partial t^2}\right)(2V_{n,m} - V_{n-1,m} - V_{n+1,m}) - \gamma_0\frac{\partial^2}{\partial t^2}(V_{n,m-1} - 2V_{n,m} + V_{n,m+1}) = \alpha\frac{\partial^2 V^2_{n,m}}{\partial t^2} - \beta\frac{\partial^2 V^3_{n,m}}{\partial t^2}, \tag{6}$$

where the linear wave speed Ω_0, the coupling coefficient γ_0, and the dispersion coefficient d_0 are given by

$$\Omega_0^2 = \frac{1}{C_0 L}, \quad \gamma_0 = \frac{C_2}{C_0}, \quad d_0 = \frac{C_S}{C_0}. \tag{7}$$

Equation (6) with coefficients (7) is the difference-differential equation governing the wave propagation in the network under consideration. In this equation, Ω_0 is the characteristic frequency of each line, γ_0 is the coupling coefficient, and d_0 is the dispersive element. As one can see from Eq. (7), all of the lines have the same characteristic fre-

quency. This is due to the fact that all of the lines are identical.

III. MODULATED WAVES IN THE COUPLED NONLINEAR DISPERSIVE TRANSMISSION LINES

Modulated waves in the network are described by considering waves with a slowly varying envelope in time and space with respect to a given carrier with angular frequency ω and wave numbers k and q. We then use the reductive perturbation method in the semidiscrete limit [7,22] which means that the dominant motion is in the n direction, and define three stretched variables in the wave frame $x=\epsilon(n-v_g t)$, $y=\epsilon m$, $\tau=\epsilon^2 t$, where ϵ is a small parameter and v_g is a constant (the meaning and expression of constant v_g will be given below). In addition, the voltage in the transmission line is expanded in the form

$$V_{n,m} = \epsilon A(x,y,\tau)\exp(i\theta) + \epsilon^2[\phi(x,y,\tau) + B(x,y,\tau)\exp(2i\theta)] + \text{c.c.}, \tag{8}$$

with $\theta=kn+qm-\omega t$, where c.c. stands for the complex conjugate. Substituting Eq. (8) into Eq. (6), we obtain different equations as power series of ϵ.

(i) The coefficient of ϵ, proportional to $\exp(i\theta)$, gives the dispersion relation

$$\omega^2(k,q) = \frac{4\Omega_0^2 \sin^2\frac{k}{2}}{1 + 4d_0 \sin^2\frac{k}{2} + 4\gamma_0 \sin^2\frac{q}{2}}. \tag{9}$$

Because the dominant motion is in the n direction, the group velocity v_g is taken to be $v_g=d\omega/dk$,

$$v_g = \frac{(\Omega_0^2 - d_0\omega^2 -)\sin k}{\omega\left(1 + 4d_0 \sin^2\frac{k}{2} + 4\gamma_0 \sin^2\frac{q}{2}\right)}. \tag{10}$$

The dispersion relation (9) shows that the angular frequency ω decreases as the coupling parameter $C_2=C_0\gamma_0$ increases. This situation is confirmed by Figs. 2(a) and 2(b) where the angular frequency ω is plotted as a function of the wave number k or q for different γ_0.

(ii) The coefficient of ϵ^2, proportional to $\exp(2i\theta)$, gives $B=\frac{\omega^2\alpha}{(d_0-\Omega_0^2)\sin^2 k+\gamma_0 \sin^2 q-\omega^2}A^2$.

(iii) The coefficient of ϵ^4, proportional to $\exp(0i\theta)$ gives $\phi=\frac{2\alpha v_g^2}{v_g^2-\Omega_0^2}|A|^2$.

(iv) The coefficient of ϵ^2, proportional to $\exp(i\theta)$, leads to

$$\left[\omega\left(1 + 4d_0 \sin^2\frac{k}{2} + 4\gamma_0 \sin^2\frac{q}{2}\right)v_g + (d_0\omega^2 - \Omega_0^2)\sin k\right]\frac{\partial A}{\partial x} + \gamma_0\omega^2 \sin q\frac{\partial A}{\partial y} = 0. \tag{11}$$

(v) From the coefficient of ϵ^3, proportional to $\exp(i\theta)$, we obtain, under the solvability conditions $q \in 2\pi\mathbb{Z}$ [the condition under which we will have a nonzero complex amplitude $A(x,y,\tau)$] and

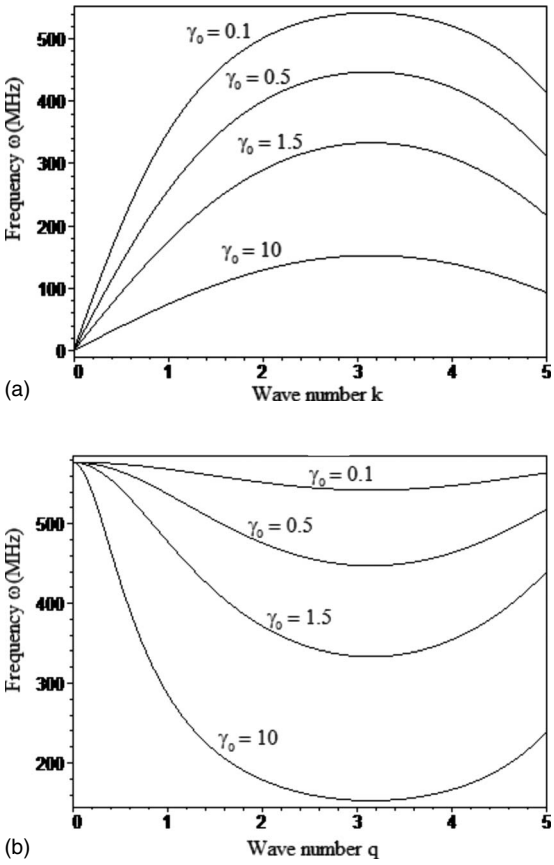

FIG. 2. The profiles of the dimensionless angular frequency ω as a function of the wave number k for $q=\pi$ (a) and as a function of the wave number q for $k=\pi$ (b) for different values of γ_0 $=0.1,0.5,1.5,10$. The coefficients $\Omega_0^2=\frac{1}{4}\times 10^{18}$ and $d_0=\frac{1}{2}$ have been used in these plots.

$$f(k) = \Omega_0^{-2}\left[v_g^2 - \Omega_0^2\cos k + d_0\left(4v_g^2 \sin^2\frac{k}{2} + 4\omega v_g \sin k + \omega^2\cos k\right) - \omega^2\gamma_0\right] = 0, \tag{12}$$

the following two-dimensional nonlinear Schrödinger equation for A:

$$i\frac{\partial A}{\partial \tau} + \frac{1}{2}P\Delta A + Q|A|^2 A = 0, \tag{13}$$

with

$$P = -\frac{\omega\gamma_0}{1 + 4d_0 \sin^2\frac{k}{2}},$$

$$Q = -\frac{\omega\left(3\beta + \frac{4\alpha^2 v_g^2}{\Omega_0^2 - v_g^2} + \frac{2\alpha^2\omega^2}{(\Omega_0^2 - d_0)\sin^2 k + \omega^2}\right)}{2\left(1 + 4d_0 \sin^2\frac{k}{2}\right)}. \tag{14}$$

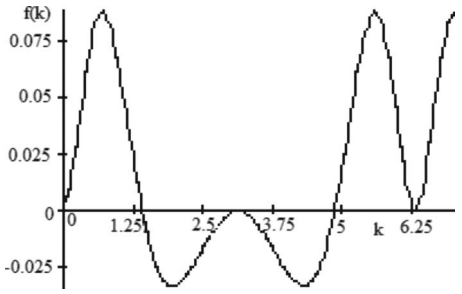

FIG. 3. Plot of $f(k)$ for the wave number $q=2\pi$ and the coefficient parameters $d_0=\gamma_0=0.5$.

From the expression (10) for the group velocity and the solvability condition $q \in 2\pi\mathbb{Z}$, it is seen that Eq. (11) is satisfied for every A.

The numbers P and Q are the dispersion and nonlinearity coefficients, respectively, of the nonlinear Schrödinger equation (13), and are negative [one can easily verify this fact by inserting the expression for v_g in Eq. (14)]. For given coefficients d_0, γ_0, and Ω_0, the dispersion coefficient P, the nonlinearity coefficient Q, and the group velocity v_g (10) are functions of the discrete wave numbers k_l, which are roots of equation $f(k)=0$, so that $\omega(k, 2\pi\mathbb{Z}) \neq 0$. In Fig. 3, $f(k)$ given by Eq. (12) is plotted as a function of the wave number k for the parameters $d_0=0.75$ and $\gamma_0=0.5$. This figure shows that $f(k)$ admits many real zeros for which $\omega(k, 2\pi\mathbb{Z}) \neq 0$.

The two-dimensional NLS equation (13) possesses a y-independent (that is, plane or line) solitary wave solution. Considering some higher-order perturbations in the y direction, we are interested in the stability of the solitary wave solution.

IV. TRANSVERSE STABILITY OF PLANE SOLITARY WAVES

It is well known that the Benjamin-Feir instabilities, exhibited by a dispersive nonlinear medium, constitute the proof of its capacity to support envelope solitons in certain propagation domains [23–25]. It follows from Eq. (13) that a continuous slowly modulated plane wave should be unstable if $PQ>0$. This instability leads to the formation of envelope pulse solitons train, plane wave solution of Eq. (13),

$$A_0(x,\tau) = \frac{A_{\max} \exp[iv_e(2x - Pv_p\tau)/4]}{\cosh[(2x - Pv_e\tau)/2S_e]}, \tag{15}$$

where v_e and v_p are the envelope and phase velocities, respectively, $S_e=\sqrt{P/Q}/\chi A_{\max}$ is the spatial soliton extension, $A_{\max}$ is the nonlinear maximum amplitude of the soliton, and χ is a positive parameter. Without loss of generality, we can take $\chi^2 \in \{1,3\}$ (we note that we can always write S_e as $S_e = \sqrt{P/Q}/\hat{\varepsilon}\tilde{A}_{\max}$, where $\tilde{A}_{\max}=\frac{\chi}{\hat{\varepsilon}}A_{\max}$ and $\hat{\varepsilon}^2 \in \{1,3\}$).

Following Ody *et al.*[26], we impose on the line soliton (15) a sinusoidal perturbation in the y direction and study the growth of this perturbation as the soliton propagates in the x direction. Using the transformations

$$x' = \frac{x}{S_e} - \frac{Pv_e}{2S_e}\tau, \quad \tau' = \tau, \quad y' = \frac{y}{S_e}, \quad u = A\exp\left(-i\frac{S_e v_e}{2}x'\right), \tag{16}$$

and dropping primes, we find that Eq. (13) and the plane wave solution (15) become

$$i\frac{\partial u}{\partial \tau} + \frac{P}{2S_e^2}\Delta u + Q|u|^2 u + P\frac{v_e^2}{8}u = 0, \tag{17}$$

$$u_0(x) = \frac{A_{\max}}{\cosh x}, \tag{18}$$

respectively.

Now, let us investigate the stability of the solitary wave solution. We may take the perturbation to be in the y direction. We follow Edy *et al.* and assume a perturbation solution to the two-dimensional (2D) NLS equation (17) of the form

$$u_p(x,y,\tau) = u_0(x) + \tfrac{1}{2}\delta[\Phi(x)\exp(iKy + \Omega\tau) + \Phi^*(x)\exp(-iKy + \Omega^*\tau)]. \tag{19}$$

In Eq. (19), δ is a small real parameter controlling the perturbation strength, $\Phi(x)$ is the perturbation complex function, K and Ω are the wave number of the perturbation and the complex frequency, respectively; the asterisk stands for the complex conjugate. Inserting Eq. (19) into Eq. (17) and keeping only the linear terms in δ leads to the following equations for the complex function $\Phi(x)$:

$$\Phi'' + \left(\frac{v_e^2 P + 8i\Omega}{4Q\chi^2 A_{\max}^2} - K^2 + \frac{6}{\chi^2}\operatorname{sech}^2 x\right)\Phi = 0. \tag{20}$$

First we note that in the limit $x \to \pm\infty$, Eq. (20), we have

$$\Phi'' + \left(\frac{v_e^2 P + 8i\Omega}{4Q\chi^2 A_{\max}^2} - K^2\right)\Phi = 0.$$

Substituting now $\Phi=\tilde{\Phi}\exp(\lambda x)$, one can see that λ satisfies the quadratic equation

$$\lambda^2 - \left(\frac{4Q\chi^2 A_{\max}^2 K^2 - v_e^2 P}{4Q\chi^2 A_{\max}^2} - i\frac{2\Omega}{Q\chi^2 A_{\max}^2}\right) = 0. \tag{21}$$

Because the roots λ_j, $j=1,2$, of Eq. (21) are distinct, the corresponding solutions of Eq. (20) are given by

$$\Phi_j(x) = \exp(\lambda_j x)h_j(x),$$

where $h_j(x)$ is the solution of equation

$$\left(\frac{d^2}{dx^2} + 2\lambda_j\frac{d}{dx} + \frac{6}{\chi^2}\operatorname{sech}^2 x\right)h_j = 0. \tag{22}$$

A. Case where $\chi^2=3$

In the case where $\chi^2=3$, we find $h_j(x)=\tanh x-\lambda_j$. Consequently,

$$\Phi_j(x) = (\tanh x - \lambda_j)\exp(\lambda_j x), \quad j=1,2. \tag{23}$$

Writing $\Omega=\Omega_r+i\Omega_i$, we find from Eq. (21),

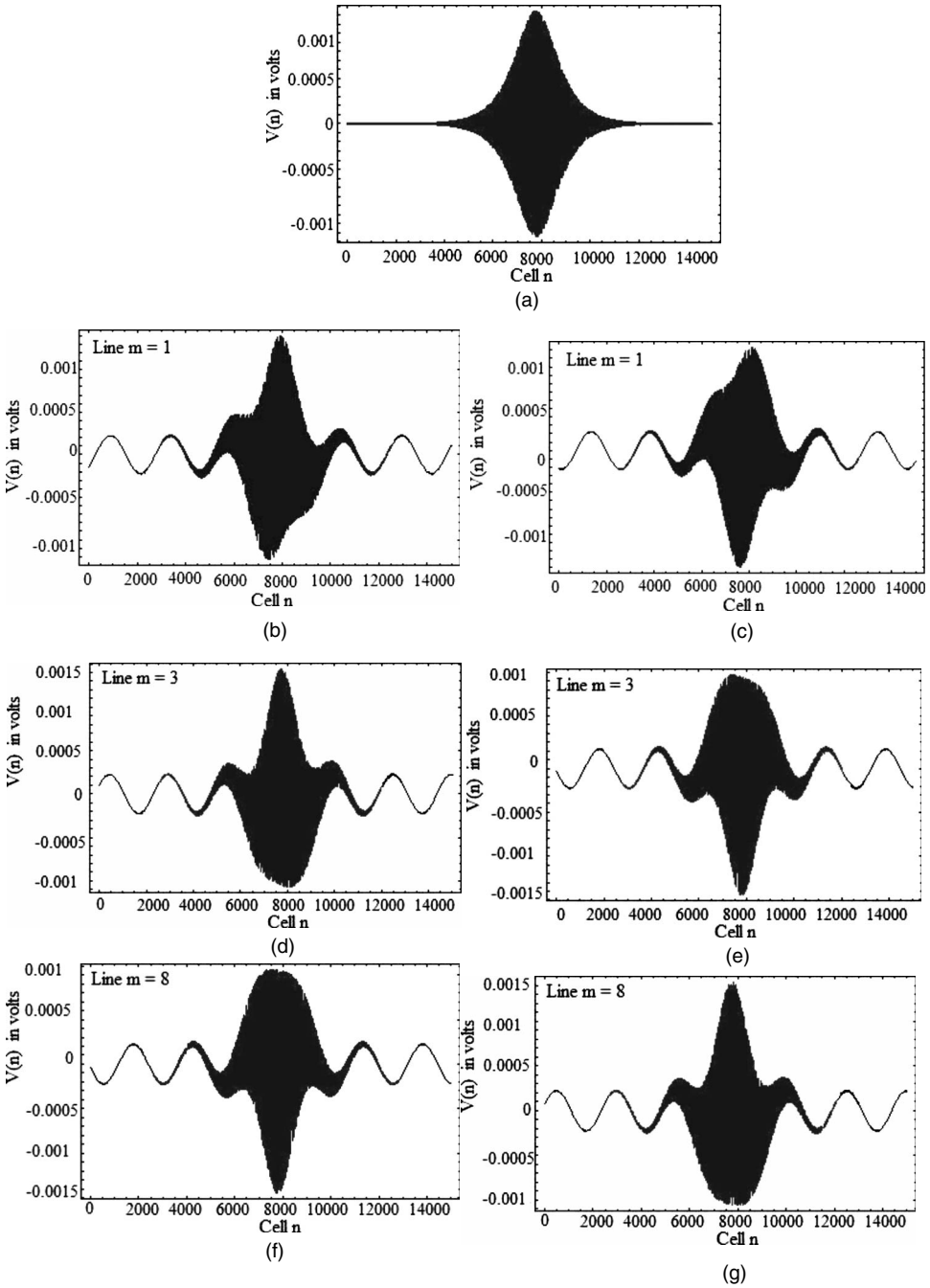

FIG. 4. Propagation of the soliton-signal voltage on the networks at a given time $t=100\ \mu s$ under the conditions of the transversal stability (27). From the top to the bottom, the plots correspond to the value of $m=1$, $m=3$, and $m=8$, respectively.

$$\lambda_j = (-1)^{j-1}(a+ib), \tag{24}$$

where a and b are defined by

$$a^2 = \frac{\alpha_0 + \sqrt{\alpha_0^2+\beta_0^2}}{2}, \quad b^2 = \frac{-\alpha_0 + \sqrt{\alpha_0^2+\beta_0^2}}{2}, \tag{25}$$

with

$$\alpha_0 = \frac{4Q\chi^2 A_{\max}^2 K^2 + 8\Omega_i - v_e^2 P}{4Q\chi^2 A_{\max}^2}, \quad \beta_0 = -\frac{2\Omega_r}{Q\chi^2 A_{\max}^2}. \tag{26}$$

It is evident that $\mathrm{Re}(\lambda_1)\mathrm{Re}(\lambda_2)\leqslant 0$. Without loss of generality, we consider that $\mathrm{Re}(\lambda_1)\geqslant 0$ and $\mathrm{Re}(\lambda_2)\leqslant 0$. In order that all the $\Phi_j(x)$, $j=1,2$, should be bounded, it is necessary and sufficient that $\mathrm{Re}(\lambda_j)=0$, i.e., $a=0$. Equation (25) then gives

$$\Omega_i \geqslant \frac{v_e^2 P}{8} - \frac{Q\chi^2 A_{\max}^2 K^2}{2}, \quad \Omega_r = 0. \tag{27}$$

Conditions (27) are the transverse stability's conditions.

Let conditions (27) be violated. Then $\mathrm{Re}(\lambda_1)$ will be positive and $\mathrm{Re}(\lambda_2)$ will be negative. If either $\Omega_r=0$ or $\Omega_r<0$, then the perturbed solution (19) that corresponds to the perturbation function $\Phi_1(x)$ will increase exponentially with $x>0$. If $\Omega_r>0$, then the perturbed solution (19) corresponding to the perturbation function $\Phi_1(x)$ will increase exponentially with both $x>0$ and $\tau>0$. With the perturbation func-

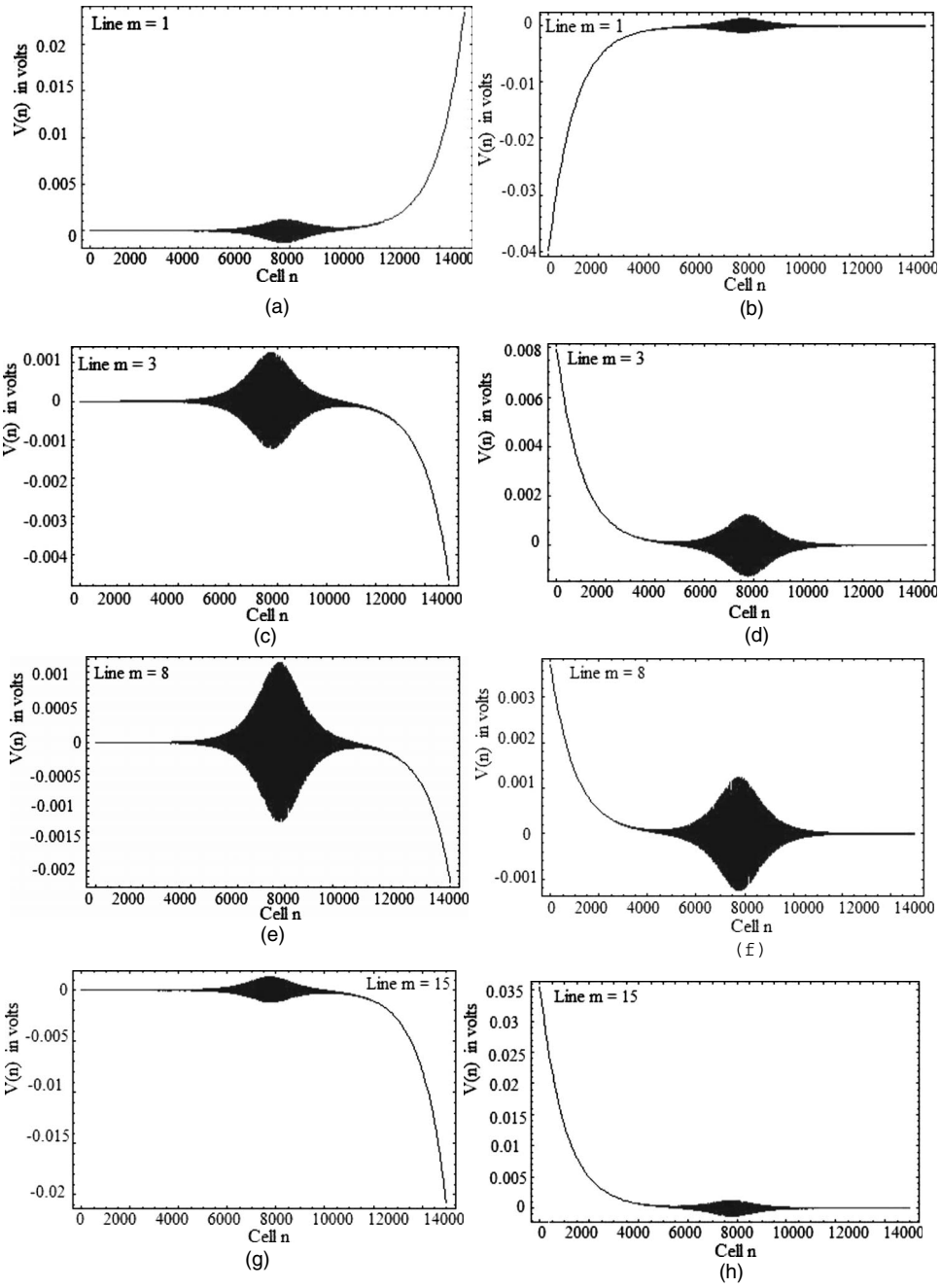

FIG. 5. Propagation of perturbed soliton-signal voltage on the different networks at a given time $t=100$ μs under the violation of conditions (27) of the transversal stability. From the top to the bottom, the plots correspond to the value of $m=1$, $m=3$, $m=8$, and $m=15$, respectively.

tion $\Phi_2(x)$, the perturbed solution (19) will remain bounded in the both x direction and τ direction for any $\Omega_r \leqslant 0$; this perturbed solution will grow exponentially in the τ direction, if $\Omega_r > 0$.

B. Case where $\chi^2=1$

In the case where $\chi^2=1$, it is helpful to write Eq. (20) in the form

$$\left(-\frac{d^2}{dx^2}+1-\frac{6}{\cosh^2 x}\right)\Phi=\omega\Phi, \tag{28}$$

$$\omega=1+\frac{v_e^2P+8i\Omega}{4Q\chi^2A_{\max}^2}-K^2. \tag{29}$$

Seeking the solutions of Eq. (28) in the form $\Phi(x)=h(x)\exp(qx)$, we find either $h(x)=-\tanh^2 x-\frac{(\omega-3)}{6}$, $q=0$ for $\omega\in\{-3,1\}$ or $h(x)=\sinh x/\cosh^2 x$, $q=0$, for $\omega=0$. We thus obtain the following solutions of Eq. (20):

$$\Phi_3(x)=\frac{1}{\cosh^2 x},\quad \Omega=i\frac{4Q\chi^2A_{\max}^2(4-K^2)+v_e^2P}{8}, \tag{30}$$

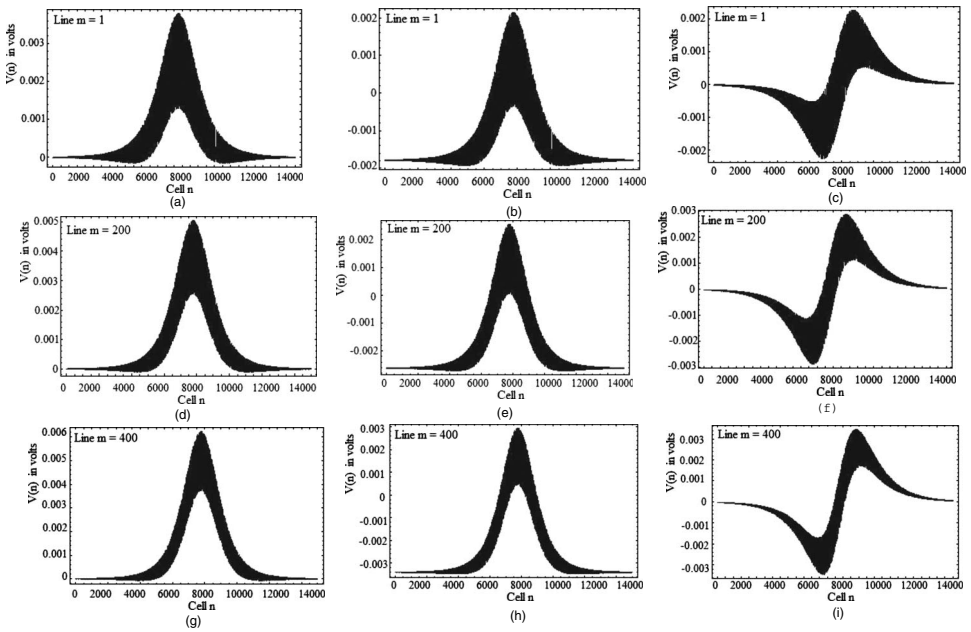

FIG. 6. Propagation of the envelope soliton on the different lines of the network in the case where $\varepsilon=1$. From the top to the bottom, the plots correspond to the value of $m=1$, $m=200$, and $m=400$, respectively.

$$\Phi_4(x) = \frac{1}{\cosh^2 x} - \frac{2}{3}, \quad \Omega = i\frac{v_e^2 P - 4Q\chi^2 A_{\max}^2 K^2}{8}, \quad (31)$$

$$\Phi_5(x) = \frac{\sinh x}{\cosh^2 x}, \quad \Omega = i\frac{4Q\chi^2 A_{\max}^2 (1-K^2) + v_e^2 P}{8}. \quad (32)$$

Thus, in the case where $\chi^2=1$, the perturbation functions $\Phi_3(x)$, $\Phi_4(x)$, and $\Phi_5(x)$ are always bounded as $x \to \pm\infty$, and the complex frequency $\Omega \in i\mathbb{R}$. Therefore, the perturbed solutions (19) with the perturbation functions and complex frequencies given by Eqs. (30)–(32) are bounded in both the x and the τ direction. The soliton solution is then stable under the transverse perturbation in the y direction.

C. Computational simulations

For the computational simulation, we use the following line parameters, $C_0=2$ pF, $C_S=1.5$ pF, $C_2=1$ pF, $L=1$ μH, $\alpha=0.21$ V^{-1}, $\beta=0.0197$ V^{-2}. The coefficients (14) of Eq. (13) are then computed for the wave number $k=1.424\,12$. In order to obtain an initial voltage profile, required as input at section $n=0$ of the system, we use expressions (23) and (30)–(32) for the perturbed solitary wave. We first revert to the laboratory coordinates n, m, and t by using Eq. (16) and the transformations $x=\epsilon(n-v_g t)$, $y=\epsilon m$, $\tau=\epsilon^2 t$. We then use formula (8) in which ϕ and B are replaced by their expressions in terms of A, and A is replaced by the perturbed solitary wave. After this is done, the input voltage as a function of m and t is obtained by setting $n=0$, specifying values of the perturbation wave number K, the complex frequency Ω, and the soliton parameters (v_e, v_p, $A_{\max}$, χ). The pulse then propagates in the dominant direction n.

Figure 4 shows the propagation of the envelope soliton on the different networks (for distinct m). In this figure, we show the signal voltage (in Volts) at a given time ($t=100$ μs) as a function of cell number n. The top figure shows the unperturbed soliton-signal accordingly to Eq. (8) with $\epsilon=0.005$. The two columns show the perturbed soliton signal given by Eq. (19) with the perturbation functions (23), for $K=454.9$, $\Omega_r=0$, $\Omega_i=0.4$, $\chi=\sqrt{3}$, $A_{\max}=0.5$, and $\delta=0.0001$. The conditions (27) of the transversal stability are then satisfied. The figures of the left-hand column correspond to the perturbation function $\Phi_1(x)$, while those of the right-hand column correspond to $\Phi_2(x)$. The plots of the two columns show that the perturbation functions $\Phi_1(x)$ and $\Phi_2(x)$ deform the propagating solitary signal.

The propagation of the envelope soliton on the different networks (for distinct m) in the case where the transversal conditions (27) are violated is shown in Fig. 5. Here, we plot the soliton-signal voltage at the given time ($t=100$ μs) as a function of cell number n. For the plots of this figure, we have used $\epsilon=0.005$, $A_{\max}=0.5$, $\delta=0.0001$, $\Omega_r=-0.2$, $\Omega_i=0.4$, $\chi=\sqrt{3}$, and $K=454.905$. The perturbed soliton signals of this figure correspond to the unperturbed soliton-signal voltage on the top of Fig. 4. The figures of the left-hand column correspond to the perturbation function $\Phi_1(x)$, while those of the right-hand column correspond to $\Phi_2(x)$. As it is seen from the plots of the two columns, the propagating perturbed solitary signal under the perturbation functions $\Phi_1(x)$ and $\Phi_2(x)$ conserves the form of the unperturbed solitary wave.

The left-hand and the right-hand columns in Fig. 4 present a symmetry, different from the one present by the two columns of Fig. 5. These two figures show that the form of the perturbed soliton at the given time depends on the line on which the wave propagates (i.e., on m).

In Fig. 6, we plot the envelope on the different networks in the case where $\chi=1$. This figure shows the soliton-signal voltage at a given time $t=100$ μs as a function of cell number n. The following solution parameters are used: $\epsilon=0.005$, $A_{\max}=0.5$, $\delta=0.01$, and $K=0.905$. The figures of the first column, the second column, and the third column correspond to the perturbation function $\Phi_3(x)$, $\Phi_4(x)$, and $\Phi_5(x)$, respectively. This perturbation functions and the corresponding

complex frequency Ω are given by Eqs. (30)–(32). The different plots of Fig. 6 show that the soliton amplitude increases with m. The plots of Fig. 6 show that the perturbation functions $\Phi_3(x)$ and $\Phi_4(x)$ perturb the propagating solitary wave in the same manner, while the perturbation function $\Phi_5(x)$ deforms the solitary wave.

V. CONCLUSION

In this paper, we have considered a system of coupled nonlinear dispersive transmission lines in which the nonlinear capacitance C is of a general form $C(V)=\frac{dQ}{dV}=C_0$ $(1-2\alpha V+3\beta V^2+\cdots)$. Using the reductive perturbation method in the semidiscrete limit, we show that the voltage for the transmission lines is described by a two-dimensional nonlinear Schrödinger equation. The exact transverse perturbation eigenfunctions and the corresponding complex frequencies are found when studying the transverse stability of solitary waves.

ACKNOWLEDGMENTS

One of the authors (E.K.) is grateful to the Instituto Nacional de Matemática Pura e Aplicada (IMPA), Rio de Janeiro, Brazil, where part of this work was done during his visit under the TWAS-UNESCO Associateship Scheme at the Centre of Excellence. He also thanks Professor B.A. Malomed for helpful discussions and critical reading of this paper.

[1] H. Washini and T. Taniuti, Phys. Rev. Lett. **17**, 996 (1966).
[2] J. N. Dinkel, C. Setzer, S. Rawal, and K. E. Lonngren, Chaos, Solitons Fractals **12**, 91 (2001).
[3] A. C. Hick, A. K. Common, and M. L. Sobby, Physica D **95**, 167 (1996).
[4] W. S. Duan, Chin. Phys. Lett. **19**, 452 (2002).
[5] W. S. Duan, X. R. Hong, Y. R. Shi, and K. P. Lv, Chin. Phys. Lett. **19**, 1231 (2002).
[6] W. S. Duan, K. P. Lv, and J. B. Zhao, Chin. Phys. Lett. **18**, 1088 (2001).
[7] T. Taniuti and N. Yajima, J. Math. Phys. **10**, 1369 (1969).
[8] K. Fukushima, M. Wadati, and Y. Narahara, J. Phys. Soc. Jpn. **49**, 1593 (1980).
[9] R. Hirota and K. Suzuki, Proc. IEEE **61**, 1483 (1973).
[10] K. Lonngren, *Solitons in Action*, edited by K. Lonngren and A. Scott (Academic, New York, 1978) pp 127–152.
[11] E. Afshari and A. Hajimiri, IEEE J. Solid-State Circuits **40**, 744 (2005).
[12] A. C. Scoot, F. Y. F. Chu, and W. Mclaughlin, Proc. IEEE **61**, 1443 (1973).
[13] T. Kakutani and N. Yamazaki, J. Phys. Soc. Jpn. **45**, 674 (1978); T. Yoshinaga and T. Kakutani, *ibid.* **49**, 2072 (1980).
[14] B. Z. Essimbi, A. M. Dikande, T. C. Kofane, and A. A. Zibi, J. Phys. Soc. Jpn. **64**, 2361 (1995).
[15] D. Yemele and T. C. Kofane, J. Phys. D: Appl. Phys. **39**, 4504 (2006).
[16] Y. A. Stepanyants, Wave Motion **3**, 335 (1981).
[17] L. A. Ostrovski, V. V. Papko, and Y. A. Stepanyants, Sov. Phys. JETP **51**, 417 (1980).
[18] E. Kengne, S. T. Chui, and W. M. Liu, Phys. Rev. E **74**, 036614 (2006).
[19] W.-S. Duan, Europhys. Lett. **66**, 192 (2004).
[20] K. Fukushima, M. Wadati, T. Kotera, K. Sawada, and Y. Narahara, J. Phys. Soc. Jpn. **48**, 1029 (1980).
[21] E. Kengne, J. Phys. A **37**, 6053 (2004).
[22] E. Kengne, Nonlinear Oscillations **6**, 346 (2003).
[23] E. J. Parkes, J. Phys. A **20**, 2025 (1987).
[24] T. B. Benjamin and J. F. Feir, J. Fluid Mech. **27**, 417 (1967).
[25] L. D. Landau, E. M. Lifshitz, *Quantum Mechanics* (Pergamon, New York, 1977).
[26] M. S. Ody, A. K. Common, and M. I. Sobhy, Eur. J. Appl. Math. **10**, 265 (1999).